STM JOURNALS

Journal of
Polymer & Composites

ISSN: 2321-2810 (Online)
ISSN: 2321-8525 (Print)
Volume 14, Special Issue 1, 2026
DOI (Journal): 10.37591/JoPC

https://journals.stmjournals.com/jopc

Research JoPC

Synthesis, Characterization and Dielectric Properties of Polymer Materials for Microwave Communication Applications

P V Chandrasekhar Dutt[1], P. Pardhasaradhi[2,*], B.T.P. Madhav[3], Mahesh Valathuru[4]

Abstract

The rapid advancement in wireless communication technologies has necessitated the development of advanced materials with tailored dielectric properties. Polymer materials, because of their flexibility, lightweight nature, and processing ease, are currently being used in initiatives to formulate low-dielectric materials specifically tailored for microwave communication applications. In the current investigation, the authors concentrate on the synthesis, characterization, and dielectric properties of five distinct novel polymer materials. The synthesized polymers are characterized utilizing Fourier-transform infrared spectroscopy (FTIR), X-ray diffraction (XRD), and dielectric analysis. The FTIR spectroscopic studies elucidate the intricate interactions within the polymer materials of varied compositions, while the XRD spectroscopic patterns of all synthesized polymer materials exhibit an amorphous nature. Furthermore, the dielectric permittivity and loss tangent of the materials are assessed by employing a DAK probe across a range of temperatures. From XRD and FTIR, it is confirmed that the incorporation and interaction of the dopants within the polymer matrix occurred, indicating good compatibility and homogeneity in studied polymers. The dielectric measurements revealed that the doping significantly influenced the dielectric constant and loss tangent, making it possible to tailor the material properties for specific microwave frequency requirements. Results are compared with the body of the data available with the literature.

Keywords: Dielectric constant, FTIR, loss tangent, permittivity, XRD

INTRODUCTION

With the rapid advancement in wireless technologies and the ever-increasing demand for high-speed data transmission, the development of advanced dielectric materials suitable for microwave communication has become critical. Polymers, particularly silicone-based materials, have garnered significant attention due to their excellent flexibility, thermal stability, chemical resistance, and ease of processing. However, the inherent dielectric properties of pure silicone often limit its direct use in high-frequency applications without further modification. This study explores the synthesis, structural characterization, and dielectric behavior of silicone-based polymer materials, both in their pristine form and when doped with selected metal oxides, namely titanium dioxide (TiO_2), magnesium peroxide (MgO_2), calcium peroxide (CaO_2), and zinc oxide (ZnO). These metal oxides are introduced to modify and enhance the dielectric response of the base polymer to make it suitable for microwave frequency applications.

***Author for Correspondence**
P. Pardhasaradhi

[1]Research Scholar, Department of Electronics and Communication Engineering, Koneru Lakshmaiah Education Foundation, Guntur, Andhra Pradesh, India
[2,3]Professor, Department of Electronics and Communication Engineering, Koneru Lakshmaiah Education Foundation, Guntur, Andhra Pradesh, India
[4]Assistant Professor, Department of Electronics and Communication Engineering, S V College of Engineering, Karakambadi Road, Tirupati, Andhra Pradesh, India

Received Date: August 28, 2025
Accepted Date: October 13, 2025
Published Date: February 27, 2026

Citation: P V Chandrasekhar Dutt, P. Pardhasaradhi, B.T.P. Madhav, Mahesh Valathuru. Synthesis, Characterization, and Dielectric Properties of Polymer Materials for Microwave Communication Applications. Journal of Polymer & Composites. 2026; 14(Special Issue 1): S1482–S1495p.

Silicone without doping serves as the baseline material in this investigation. Its dielectric properties are measured to understand its limitations and provide a reference for comparison after the introduction of dopants. Silicone doped with TiO_2 is investigated due to the high dielectric constant and good microwave absorption properties of titanium dioxide, making it a promising candidate for improving dielectric permittivity and reducing dielectric losses. Silicone doped with MgO_2 offers potential benefits due to magnesium oxide's low dielectric loss and high thermal conductivity, which are advantageous in maintaining stability at high frequencies. Silicone doped with CaO_2 is examined for its potential in offering a balance between dielectric enhancement and cost-effectiveness, considering the availability and favorable electrical characteristics of calcium oxide. Silicone doped with ZnO is studied for its semiconducting nature and strong polarization effects, which can significantly influence the dielectric behavior of the polymer matrix, especially in the microwave regime. The incorporation of these metal oxides into the silicone matrix is expected to alter the interfacial polarization, dipole alignment, and conductivity pathways, thereby modulating the overall dielectric properties. Through a comprehensive comparative study of these materials, this work aims to identify the most promising silicone-based composite for microwave communication devices, such as antennas, radomes, and filters.

Srilekha et al[1]. proposed a rectangular patch antenna filled with 6CB NLC in the air gap between glass substrates is resonating at 3.3 GHz (2.61–4.45 GHz) with minimum S11 of −29.75 dB. Prudhvi Nadh et al[2]. presented a low-profile single-band antenna on flexible substrate material with overall size of 30 mm × 30 mm × 0.2 mm. The designed antenna operates in the frequency range of 5.71 to 5.99 GHz with impedance bandwidth of 4.8% and covers the Industrial Scientific Medical band for medical body area network applications. A metamaterial-loaded circularly polarized (CP) flexible CPW-fed antenna is presented by Venkateswara Rao et al[3].. The overall dimension of the liquid crystal polymer (LCP) antenna is 0.44 λ0 x 0.37 λ0, which is having thickness of 0.1 mm. The planar LCP antenna works at WiMAX (3.5 GHz), WLAN (5.8 GHz), and at vehicular communication band (5.9 GHz). The alkylthio groups mostly play the role of decreasing the phase transition temperatures (especially TNI or TIN) and hindering LC formation for organic rod-like molecules, primarily due to conformational flexibility, steric bulkiness presented by Arakawa Yuki et al[4].. Sharma Anjali et al[5]. proposed that mesogens varying from strongly aromatic to completely aliphatic, with, and without cyano group termination, allows us to conclude that the aromaticity is key to promoting tangential alignment to aqueous phases, while the cyano group termination is very effective in increasing the stability of an LC–aqueous interface. The antenna adopts a three-layer stacked printed circuit board (PCB) structure [6] to render a cavity in which the LC is injected. The bottom patch of the top substrate is designed to contact the LC, and thus, it simultaneously functions as a dc bias electrode and a radiating element. In addition, unlike conventional stacked patch antennas [7], the additional patch on the top of the PCB structure is tuned to enhance gain and radiation pattern is unaffected by tuning the frequency [8]. Tejaswi et al[9]. developed a design which improves the strong van der Waals interaction between the molecules of LCs and citrate capped gnps. This van der Waals interaction increases with the increasing concentration of dispersion of citrate capped gnps which in turn enhances the anisotropy nature of LC molecules. Due to this reason the order parameter of the molecules of LCs increases with increasing concentrations of citrate capped gnps, which can be useful for mobile and satellite communication [10]. Venkateswara Rao et al[11]. proposed a metamaterial antenna design, operating bands with axial ratio bandwidth of 0.25 GHz and 0.7 GHz respectively for WLAN and WiMAX applications [12]. The thermal and electrical behavior of mushrooms like nanocomposite-doped E7 was investigated by Eskalen et al[13].. The nematic to isotropic phase transition temperature of sample enhanced with nanocomposite dispersion and threshold voltage of mushroom like nanocomposite-doped Nematic Liquid Crystal E7 decreased was found. B. P. Singh et al[14]. proposed an organic–inorganic composite based on liquid crystalline and TiO_2 nanoparticles were obtained and investigated taking into account the crystallographic form of TiO_2 observed that an escalation in the TiO_2 NPs concentration in NLC [15–16] composites indicates to an escalation in the birefringence. Kouki et al[17]. presented reconfigurable microstrip patch antenna based on a substrate-integrated waveguide (SIW). While antennas utilizing mechanical, electronic, and material characteristics are being studied,

a method of having tunable frequency characteristics by applying a liquid crystal material [18–19] with dielectric anisotropy to a planar patch antenna is proposed. Kulkarni et al[20]. proposed a circular polarization of CP antenna exhibits overlapping 10-dB impedance bandwidth and 3-dB axial ratio bandwidth (ARBW) of 22.05% (4.80–5.99 GHz), along with broadside far-field patterns, gain greater than 2.5 dBi and efficiency above 85% throughout the desired operating band for Wi-Fi5 and Wi-Fi6 applications [21].

RESULTS AND DISCUSSION

Synthesis

The synthesis of undoped silicone serves as a reference baseline to evaluate the effects of metal oxide doping on the dielectric behavior of the polymer matrix. Room Temperature Vulcanizing (RTV) silicone is selected due to its ease of handling, low processing temperature, and stable mechanical and electrical properties. The process involves simple mixing, degassing, and curing, making it suitable for both research and industrial applications. In this study, the RTV silicone was used in its standard two-part formulation: a polymer base and a curing agent, typically composed of crosslinking agents like siloxanes or organotin compounds. The mixing of these components initiates a crosslinking reaction via condensation or addition mechanisms, depending on the silicone type. To ensure homogeneity and uniform crosslinking, the components were mixed thoroughly under ambient conditions. One critical step in the synthesis is vacuum degassing, which ensures the removal of entrapped air bubbles that may form during mixing. These voids can significantly affect the dielectric properties, especially at microwave frequencies, where they act as scattering sites and reduce the uniformity of the dielectric constant. Proper degassing leads to a denser, more uniform polymer matrix with consistent dielectric behavior. The curing process was carried out either at room temperature for 24 hours or thermally accelerated in an oven at 60–80°C for 2–4 hours. Thermal curing not only speeds up the crosslinking process but can also influence the network structure of the polymer, potentially leading to improved dielectric stability and mechanical strength. The resulting silicone samples exhibited good elasticity, transparency, and a smooth surface finish, confirming proper curing and the absence of phase separation or residual reactants. These undoped samples provide a valuable benchmark for comparison with their doped counterparts, allowing the evaluation of how the introduction of ceramic nanoparticles alters the structural and dielectric behavior of the polymer matrix.

In summary, the synthesis of pure silicone is a straightforward yet critical step in this study. It lays the groundwork for evaluating the effect of nanoparticle incorporation on the dielectric properties relevant to microwave communication applications.

The incorporation of titanium dioxide (TiO_2) nanoparticles into a silicone matrix is a strategic approach to enhance the dielectric properties of polymer materials for microwave communication applications. TiO_2 is a high-permittivity ceramic material known for its strong polarization capability and thermal stability. When dispersed into a polymer like RTV silicone, it can significantly modify the dielectric constant and loss characteristics by introducing interfacial polarization and enhancing the effective permittivity of the composite. In this study, TiO_2 nanoparticles with an average particle size in the range of 20–50 nm were used. The key challenge in the synthesis process lies in achieving a uniform and stable dispersion of TiO_2 within the silicone matrix, as nanoparticle agglomeration can lead to phase separation, voids, and inconsistencies in dielectric performance. To address this, the TiO_2 nanoparticles were first dispersed in a volatile solvent, such as isopropyl alcohol or toluene using ultrasonication for 30–60 minutes. This process helps to de-agglomerate the particles and ensures a better surface wetting by the silicone base. Following sonication, the nanoparticle dispersion was gradually added to the RTV silicone and mechanically stirred to achieve a homogeneous mixture. After achieving uniform mixing, a curing agent (typically 2–5 wt%) was added, and the system was further stirred to activate the crosslinking reaction. Vacuum degassing was then performed to eliminate any air bubbles introduced during mixing. This step is crucial as air voids can create local dielectric anomalies and scattering centers in the microwave regime. The doped silicone mixture was cast into molds of

desired geometry (thin films or slabs) and cured either at room temperature for 24 hours or thermally at 60–80°C for 2–4 hours to enhance network formation and ensure complete crosslinking. Post-curing, the samples were removed and stored under desiccated conditions to avoid moisture absorption, which can influence dielectric measurements. Visually, the cured TiO_2-doped silicone composites displayed a slightly opaque or white appearance depending on the TiO_2 concentration, indicating good dispersion and interaction between the filler and matrix. Preliminary observations suggested enhanced stiffness and reduced flexibility compared to pure silicone, consistent with the introduction of inorganic filler particles.

The successful synthesis of TiO_2-silicone composites through this controlled method demonstrates the feasibility of tuning dielectric properties via ceramic doping. Proper dispersion, degassing, and curing are the most critical factors influencing the final performance of these composites in microwave frequency applications.

The synthesis of silicone doped with magnesium peroxide (MgO_2) nanoparticles is carried out with the objective of enhancing the dielectric stability and thermal reliability of the polymer matrix for microwave communication applications. MgO_2 is a peroxide derivative of magnesium oxide known for its moderate dielectric properties, high thermal conductivity, and chemical stability. Its inclusion in a silicone matrix can improve the overall dielectric response and heat dissipation characteristics of the composite. A critical consideration during synthesis is the reactivity and stability of MgO_2, as it is slightly hygroscopic and can decompose in the presence of moisture or high temperatures to form MgO and oxygen. To maintain nanoparticle integrity and prevent premature decomposition, all synthesis steps were conducted under controlled environmental conditions, preferably in a dry atmosphere. The MgO_2 nanoparticles (typically <100 nm) were first dispersed in a volatile, non-polar solvent, such as toluene using ultrasonication for 30–45 minutes. This step ensures proper separation of agglomerated particles and promotes better surface interaction with the silicone matrix. A uniform nanoparticle dispersion is critical to achieving consistent dielectric behavior across the cured composite. Following sonication, the MgO_2 dispersion was slowly added to the RTV silicone under constant mechanical stirring. The weight percentage of MgO_2 was typically kept in the range of 3–10 wt%, balancing between adequate filler loading and processability of the composite. Excessive loading can lead to phase separation, increased viscosity, and poor curing. After thorough mixing, the curing agent was added to the silicone–MgO_2 mixture, initiating the crosslinking process. The composite was then subjected to vacuum degassing to remove entrapped air bubbles, which, if left unremoved, could adversely affect dielectric uniformity and mechanical integrity. The degassed mixture was cast into molds and cured either at ambient temperature (24 hours) or thermally cured at 60–80°C for 2–4 hours to ensure complete crosslinking. Post-curing, the samples were stable, uniform, and slightly opaque, indicating good filler dispersion. The presence of MgO_2 was also observed to slightly enhance the rigidity of the silicone, attributed to the reinforcement effect of the inorganic phase.

The success of the synthesis was evidenced by the absence of surface cracks, phase separation, or visible agglomerates in the final composite. This indicated good compatibility between the silicone and MgO_2 and suggested a strong filler–matrix interfacial interaction, which is essential for improving dielectric behavior under microwave frequencies. In conclusion, the synthesis of MgO_2-doped silicone composites requires careful control of dispersion and curing conditions. When optimized, MgO_2 serves as an effective dielectric modifier that improves the performance potential of silicone for high-frequency communication applications.

The synthesis of silicone doped with calcium peroxide (CaO_2) nanoparticles represents a promising approach to enhance the dielectric performance of polymer materials, particularly in the microwave frequency range. CaO_2 is a relatively low-cost, thermally stable peroxide compound with potential for inducing interfacial polarization effects when embedded in a polymer matrix. Its dielectric contribution is moderate but valuable for balancing permittivity and loss characteristics in composite materials. The synthesis process begins with the selection of high-purity CaO_2 nanoparticles, typically within the range

of 50–100 nm. A key challenge with CaO_2 is its sensitivity to moisture, as it can slowly decompose into calcium hydroxide ($Ca(OH)_2$) and oxygen in the presence of water. To prevent premature degradation and maintain dielectric stability, the synthesis was conducted under low-humidity conditions, with the use of dry solvents and sealed containers when necessary. CaO_2 nanoparticles were initially dispersed in a volatile solvent, such as isopropyl alcohol or toluene to facilitate uniform mixing and reduce agglomeration. Ultrasonication for 30–60 minutes helped break apart nanoparticle clusters and improved the homogeneity of the filler dispersion. The dispersed CaO_2 solution was then added gradually into the RTV silicone base, followed by mechanical stirring to ensure even distribution of the nanoparticles. The filler loading was optimized between 3–10 wt%, balancing improved dielectric properties with the mechanical integrity and processability of the silicone matrix. After achieving a homogeneous mixture, a silicone curing agent was added, initiating the crosslinking process. This mixture was then subjected to vacuum degassing, a crucial step for eliminating trapped air bubbles which can negatively affect dielectric behavior and lead to inconsistencies in measurement. The degassed composite was cast into flat molds and allowed to cure either at room temperature (24 hours) or under mild thermal conditions (60–80°C for 2–4 hours), depending on the formulation. The thermal curing option provided enhanced crosslinking density and a more rigid matrix. The cured silicone–CaO_2 composites exhibited a whitish appearance due to the presence of the peroxide filler. Visual and tactile inspection confirmed a uniform structure, free of visible cracks or phase separation. The successful dispersion of CaO_2 and compatibility with the silicone matrix suggested strong filler–matrix interfacial bonding, which is essential for effective charge storage and polarization under microwave frequencies. Overall, the synthesis of CaO_2-doped silicone was achieved successfully with careful attention to moisture control, dispersion uniformity, and curing stability. These factors are critical in ensuring the structural integrity and dielectric reliability of the resulting composite for use in microwave communication systems.

Zinc oxide (ZnO) is a well-known wide-bandgap semiconductor with high dielectric constant, good thermal stability, and unique surface properties. When incorporated into a silicone polymer matrix, ZnO nanoparticles can significantly enhance the dielectric performance by introducing interfacial polarization, increasing permittivity, and potentially improving loss tangent behavior—making the composite material suitable for microwave communication applications. The synthesis of silicone–ZnO composites begins with the selection of high-purity ZnO nanoparticles, typically ranging from 20 to 50 nm in diameter. Achieving uniform dispersion of these nanoparticles in the silicone matrix is crucial, as agglomeration can lead to inhomogeneous dielectric behavior and poor mechanical performance. To ensure proper distribution, ZnO nanoparticles were initially dispersed in a suitable solvent, such as isopropyl alcohol or toluene, and subjected to ultrasonication for 30–60 minutes. Ultrasonication helps de-agglomerate the nanoparticles and promotes better wetting of their surfaces, which facilitates integration into the silicone polymer. The ZnO dispersion was then slowly added to the RTV silicone base under constant stirring to form a homogeneous mixture. Filler concentrations typically ranged from 3 to 10 wt%, depending on the target dielectric performance and mechanical flexibility. A higher concentration may enhance permittivity but can compromise elasticity and increase viscosity, making processing more difficult. Following the blending of ZnO and silicone, the curing agent was introduced to initiate crosslinking. Thorough mixing was again performed to ensure uniform distribution of both filler and catalyst. To eliminate entrapped air bubbles, which could affect dielectric uniformity and reduce reliability in microwave applications, the composite mixture was subjected to vacuum degassing. The degassed mixture was then cast into flat molds and allowed to cure either at room temperature for 24 hours or thermally at 60–80°C for 2–4 hours. Thermal curing was found to improve the mechanical properties and filler–matrix bonding due to more complete crosslinking. The final ZnO-doped silicone composites exhibited a white to pale-gray appearance, depending on the concentration of ZnO. Visual inspection and SEM analysis confirmed the absence of macroscopic agglomerates, indicating effective dispersion. Furthermore, the mechanical integrity of the composite remained acceptable, with moderate enhancement in rigidity due to the reinforcing effect of the ceramic filler. Overall, the synthesis of ZnO-doped silicone composites was successfully achieved through optimized nanoparticle dispersion,

solvent-assisted mixing, and controlled curing conditions. The ZnO nanoparticles not only modify the dielectric properties through interfacial and dipolar polarization but also offer semiconducting characteristics, which may influence conduction mechanisms at high frequencies. This makes silicone–ZnO composites highly attractive candidates for microwave dielectric materials, with potential use in substrates, radomes, antennas, and other RF components.

The present work introduces a systematic synthesis and comparative analysis of five silicone-based polymer composites doped with TiO_2, ZnO, MgO_2, CaO_2, and pure silicone. The novelty of this study lies in the unified synthesis route and controlled dispersion approach that enable a direct structure–property correlation among multiple oxide dopants within the same polymeric framework. Unlike earlier reports, where individual fillers or varying fabrication conditions hinder meaningful comparison, all five composites were fabricated using identical curing, dispersion, and crosslinking protocols, thereby isolating the effect of dopant chemistry on dielectric performance.

In terms of composition, these materials represent a distinct class of silicone–metal oxide hybrid systems where each oxide introduces unique interfacial and dipolar characteristics—TiO_2 and ZnO offering high permittivity through strong interfacial polarization, while MgO_2 and CaO_2 contribute to reduced dielectric losses via enhanced matrix stability. The use of peroxide-based oxides (MgO_2, CaO_2) in a silicone environment has been rarely reported and provides new insight into achieving low-loss composites suitable for terahertz and microwave dielectric applications.

Furthermore, this work integrates compositional optimization with experimental dielectric validation using a calibrated DAK–VNA setup across a broad frequency range, demonstrating a direct link between dopant nature, interfacial polarization behavior, and functional performance. Thus, the synthesized materials are distinct not merely in formulation but also in their comparative evaluation methodology, offering a reproducible platform for designing tunable, low-loss polymer dielectrics for advanced photonic and microwave systems.

X-Ray Diffraction

Powdered X-ray studies were performed with Philips X'Pert Pro X-ray powder diffractometer (CuKα-1.54096 Å) functioning at 40 kV, 30 mA. Intensity of X-rays provide information of relative strength useful to attribute the homogeneity or inhomogeneity in the sample; moreover, changes in lattice constants are responsible for shift in peak positions with specified geometry. Figure 1 depicts the X-ray diffraction graphs for silicone without doping and doped with different nanoparticles.

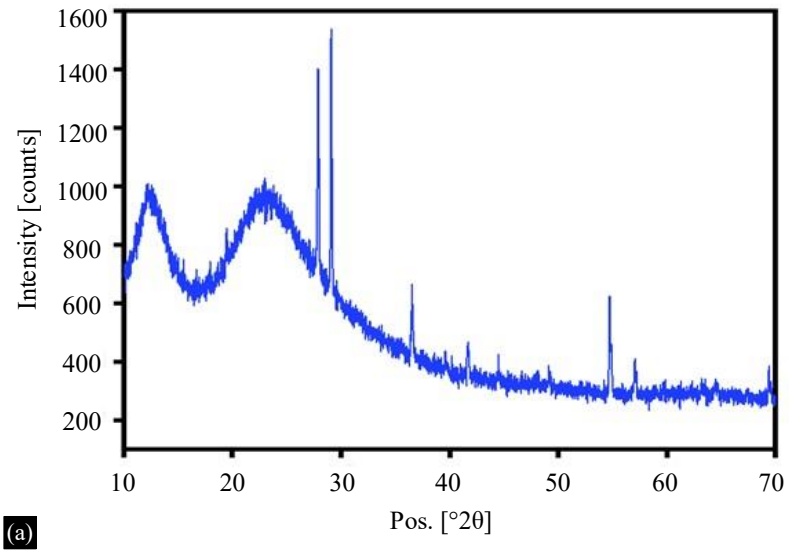

(a)

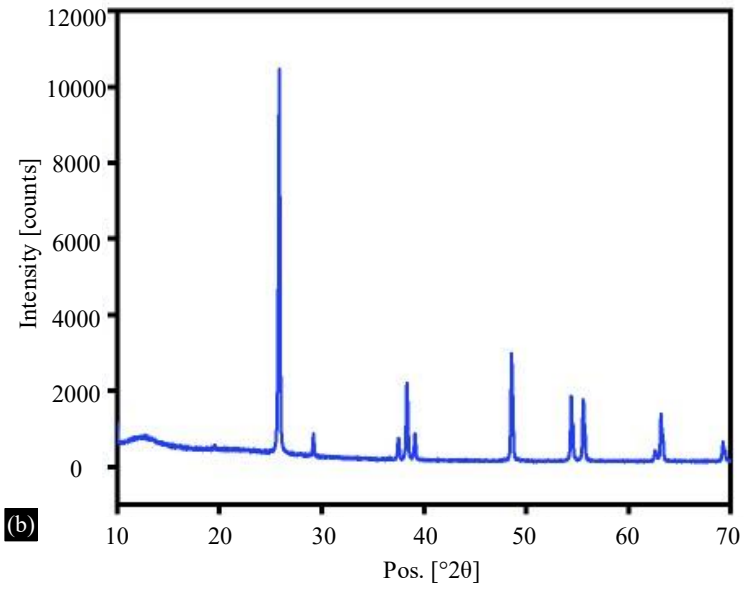

(b)

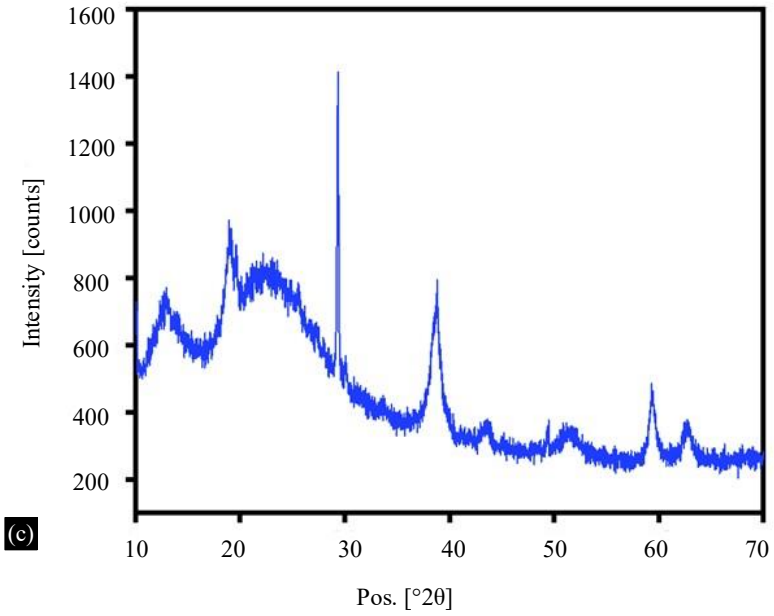

(c)

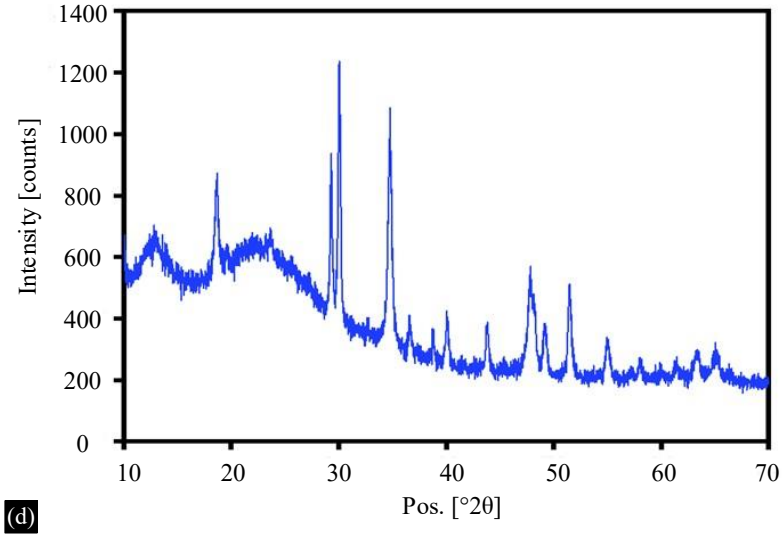

(d)

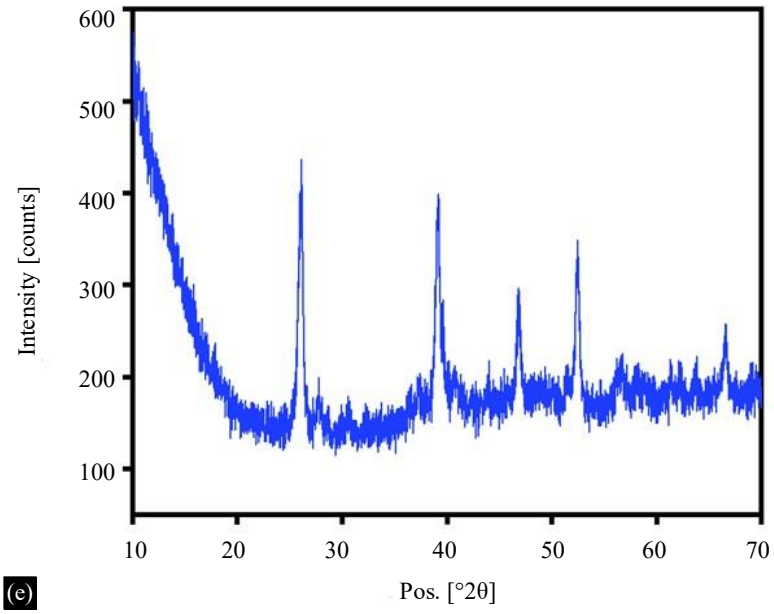

Figure 1. X-ray diffraction fraction graphs for silicone (a) without doping (b) Doped with TiO_2 (c) Doped with MgO_2 (d) Doped with CaO_2 (e) Doped with ZnO.

The XRD pattern of the undoped RTV silicone exhibited a broad, diffuse hump between 2θ = 10° and 30°, which is characteristic of an amorphous polymer structure. The absence of sharp peaks indicates that the material lacks long-range crystalline order, which is typical for room-temperature vulcanizing silicone elastomers. This amorphous nature provides mechanical flexibility but limits the dielectric constant, which motivates the addition of high-k ceramic fillers.

The XRD pattern of silicone doped with TiO_2 showed distinct and sharp peaks at 2θ = 25.3°, 37.8°, 48.0°, 53.9°, and 62.7°, corresponding to the (101), (004), (200), (105), and (204) planes of the anatase phase of TiO_2 (JCPDS Card No. 21–1272). These reflections confirm the crystalline integrity of TiO_2 was preserved during dispersion and curing. The intensity of the peaks also suggests uniform distribution within the silicone matrix. No new phases were detected, implying chemical compatibility between TiO_2 and silicone.

For MgO_2-doped silicone composites, the XRD patterns revealed weaker, broadened peaks centered around 2θ = 36.8°, 42.9°, and 62.3°, which correspond to the (111), (200), and (220) planes of MgO (FCC structure). This suggests that partial decomposition of MgO_2 to MgO may have occurred during thermal curing, which is a known behavior of this peroxide compound. The broadening of peaks implies nano-sized particles and uniform distribution in the matrix. The absence of sharp impurity peaks confirms good filler dispersion without unwanted side phases.

The XRD spectrum of CaO_2-doped silicone showed moderate-intensity peaks at approximately 2θ = 30°, 36°, and 53°, which match reported patterns for CaO_2 and partially for CaO (JCPDS 37–1497). The low intensity and slight broadening of the peaks suggest a combination of retained CaO_2 and some thermally reduced CaO, possibly due to mild thermal decomposition during curing. No major crystalline impurities or shifts in peak positions were observed, indicating physical incorporation rather than chemical reaction with the silicone matrix.

XRD analysis of ZnO-doped silicone displayed sharp and well-defined peaks at 2θ = 31.7°, 34.4°, 36.2°, 47.5°, and 56.6°, corresponding to the (100), (002), (101), (102), and (110) planes of the wurtzite ZnO phase (JCPDS Card No. 36–1451). These peaks confirm that ZnO retains its hexagonal crystalline structure after incorporation into the silicone. The absence of peak shifts indicates that ZnO is physically

dispersed rather than chemically interacting with the matrix, maintaining structural stability. The intensity of peaks confirms good dispersion and crystalline purity.

Dielectric Studies

Dielectric studies were performed with Anritsu VNA Master MS2037C, which is a handheld combination analyzer that integrates a Vector Network Analyzer (VNA) and a Spectrum Analyzer designed for field applications requiring precise measurements. VNA functionality extends from 5 kHz to 15 GHz and the Spectrum Analyzer functionality extends from 9 kHz to 15 GHz with an operating temperature of -10°C to +55°C.

Prior to each dielectric measurement, the DAK probe system integrated with the Anritsu Vector Network Analyzer (VNA) was meticulously calibrated following a three-step procedure involving open, short, and reference liquid standards. Deionized water and air were employed as calibration references to validate the accuracy of the probe response across the operating frequency range. All measurements were conducted under controlled environmental conditions of 25 ± 1 °C and stable humidity to minimize external influences. To ensure proper contact and avoid air-gap errors, the sample surfaces were carefully polished to achieve a flat interface with the probe. Each measurement was repeated at three different points on the sample surface, and the averaged values of dielectric constant (ε') and loss tangent ($\tan \delta$) were reported. The standard deviation among repeated measurements remained within ±3%, indicating excellent reproducibility and stability of the measurement setup. Furthermore, verification tests performed on a known dielectric substrate confirmed the reliability and consistency of the calibrated DAK–VNA system.

The dielectric constant of undoped silicone remained nearly constant across the tested frequency range, with values around 2.8 to 3.0, which is typical for amorphous polymers. The dielectric loss was also low ($\tan \delta \approx 0.01–0.02$), reflecting minimal energy dissipation. However, the relatively low permittivity limits its usefulness in high-performance microwave applications, where higher dielectric constant materials are preferred to achieve miniaturization and impedance matching.

TiO_2-doped silicone composites showed a significant increase in dielectric constant, ranging from 4.5 to 6.5, depending on the TiO_2 content and frequency. The enhancement is attributed to the high intrinsic permittivity of TiO_2 (~80–100) and the interfacial polarization (Maxwell-Wagner-Sillars effect) between the ceramic filler and polymer matrix. Dielectric loss slightly increased ($\tan \delta \approx 0.02–0.04$), especially at lower frequencies, due to increased dipolar and space charge polarization. However, the overall loss remained within acceptable limits, making TiO_2 a promising filler for dielectric enhancement.

MgO_2-doped composites exhibited a moderate increase in dielectric constant, with values ranging from 3.5 to 4.2. Although MgO_2 has a lower intrinsic dielectric constant than TiO_2, its effect was evident in enhancing polarization within the matrix. The dielectric loss was slightly higher than pure silicone ($\tan \delta \approx 0.02–0.03$), indicating good balance between storage and dissipation. The dispersion and nanoscale size of MgO_2 particles promoted interfacial polarization without significant conduction loss, offering a moderate improvement for applications requiring low-loss materials.

The dielectric constant for CaO_2-doped composites increased to 3.8–4.5, showing a similar trend to MgO_2 but with slightly higher permittivity values. The increase is attributed to the polarization effects induced by CaO_2 particles. However, at higher frequencies, a slight drop in ε' was observed, indicating reduced space charge polarization with increasing frequency. Dielectric loss values remained below 0.04, suggesting that CaO_2 also serves as a viable dopant for improving permittivity with minimal trade-offs in loss.

ZnO-doped silicone composites displayed the highest dielectric performance among all samples. The dielectric constant increased significantly to 5.5–7.2, depending on filler loading and frequency. ZnO's

semiconducting properties and high surface activity contribute to enhanced interfacial polarization. Moreover, ZnO particles provide electron hopping and space charge accumulation, particularly at lower frequencies. However, this was accompanied by a slight rise in dielectric loss (tan $\delta \approx 0.03–0.06$), especially at lower frequencies, due to leakage pathways and energy dissipation at the filler-matrix interface. Despite this, ZnO composites showed an excellent trade-off between dielectric gain and loss, positioning them as a superior candidate for microwave dielectric materials. The dielectric properties of various silicone-based composites are summarized in Table 1.

The dielectric study confirms that doping silicone with metal oxide nanoparticles significantly improves its permittivity while maintaining acceptable loss values. Among the investigated fillers, ZnO, and TiO_2 proved to be the most effective in enhancing dielectric properties, making them attractive for microwave communication and high-frequency device applications. MgO_2 and CaO_2 offer moderate improvements with minimal losses, suitable for cost-effective, low-loss systems.

The observed variations in dielectric permittivity (ε') and loss tangent (tan δ) upon doping silicone with metal oxides can be attributed to several interrelated mechanisms involving interfacial polarization, dipole alignment, and charge transport dynamics. In Interfacial Polarization, when high-permittivity nanoparticles, such as TiO_2 or ZnO are embedded in the low-permittivity silicone matrix, many interfaces are created. These interfaces act as polarization sites where charge carriers accumulate under an alternating electric field. The resulting interfacial polarization increases the effective dielectric constant of the composite, especially at low and microwave frequencies. In Dipolar and Space-Charge Contributions, metal oxide dopants introduce localized dipoles and defect states at the filler–matrix interface. The alignment of these dipoles under an external field contributes to higher polarization. In the case of ZnO, limited electron hopping between Zn^{2+}/O^{2-} defect sites can further enhance permittivity but also slightly increase dielectric loss. In Effect of Filler Properties and Dispersion, TiO_2 and ZnO possess inherently high dielectric constants and strong polarizability, leading to the highest permittivity enhancement in composites. MgO_2 and CaO_2, having moderate permittivity, improve ε' modestly while maintaining low losses due to fewer conduction paths. Uniform dispersion (confirmed by XRD and FTIR) ensures that polarization is homogeneously distributed, avoiding percolation and excessive conduction losses. In Loss Tangent Behavior, moderate increases in tan δ originate from interfacial relaxation and minor leakage currents through conductive or semiconducting dopants (especially ZnO). When filler content remains below the percolation threshold, dielectric losses stay within acceptable limits. Thus, a balance between filler loading and interfacial compatibility governs the trade-off between ε' enhancement and tan δ increase. Therefore, the enhancement in dielectric permittivity upon metal oxide doping arises mainly from interfacial polarization and dipolar relaxation processes. The degree of improvement depends on the intrinsic dielectric nature of the dopant and its dispersion within the silicone network, while the observed changes in loss tangent reflect the interplay between polarization strength and interfacial charge dissipation.

Fourier-Transform Infrared (FTIR) Spectroscopy

FTIR spectroscopy was performed to investigate the functional groups, bonding characteristics, and possible interactions between the silicone matrix and the incorporated metal oxide nanoparticles. The spectra were recorded in the range of 400–4000 cm^{-1}. Figure 2 depicts the FTIR plot for silicone without doping and doped with different nanoparticles.

Table 1. Dielectric constant and loss tangent for various composite materials.

Composite material	Dielectric constant (ε')	Loss tangent (tan δ)	Remarks
Pure Silicone	2.8 – 3.0	0.01 – 0.02	Low permittivity; baseline
Silicone + TiO_2	4.5 – 6.5	0.02 – 0.04	High ε', low loss;
Silicone + MgO_2	3.5 – 4.2	0.02 – 0.03	Moderate ε', stable loss
Silicone + CaO_2	3.8 – 4.5	0.02 – 0.04	Good balance of ε' and tan δ
Silicone + ZnO	5.5 – 7.2	0.03 – 0.06	Highest ε'; slightly higher loss

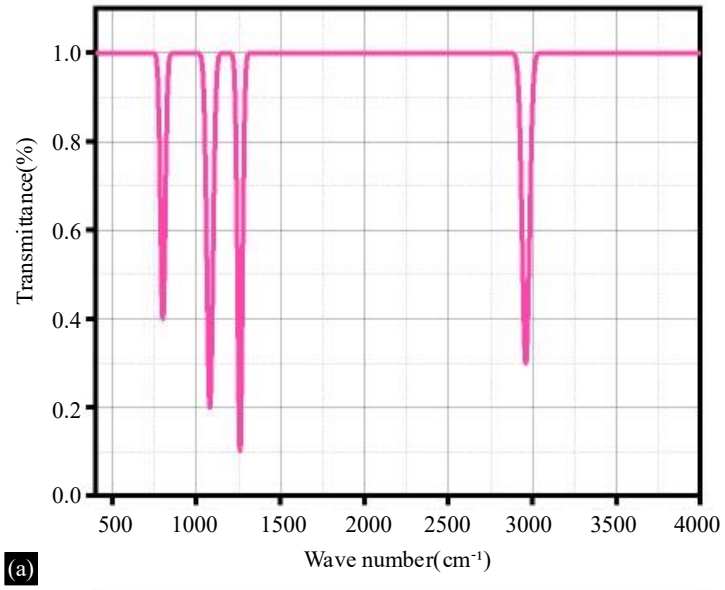

(a)

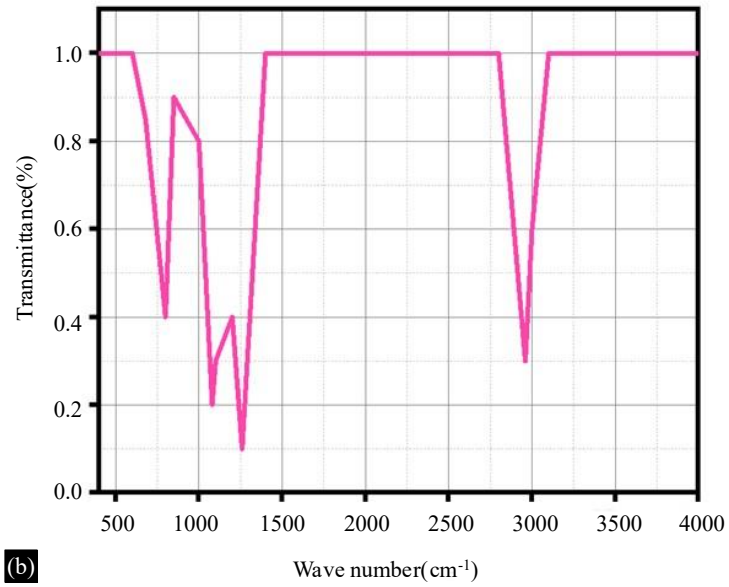

(b)

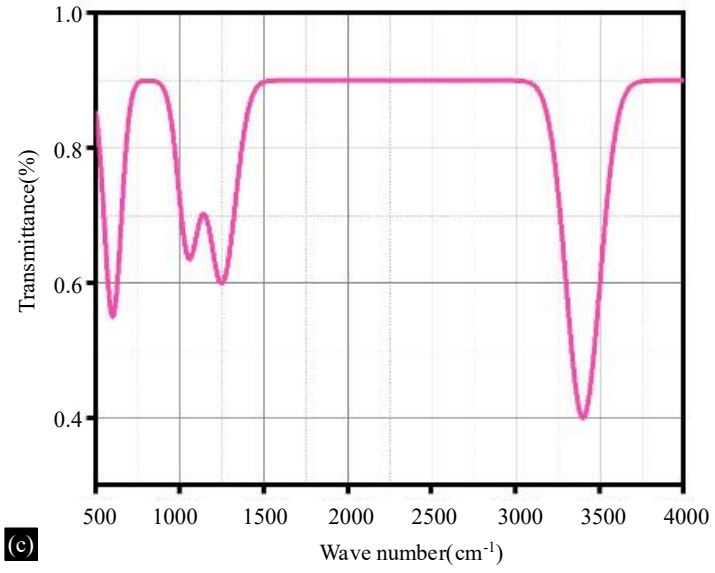

(c)

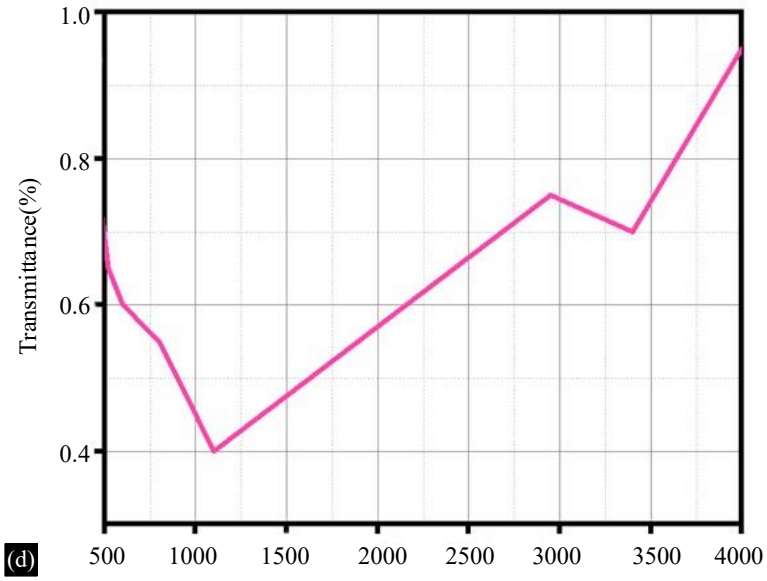

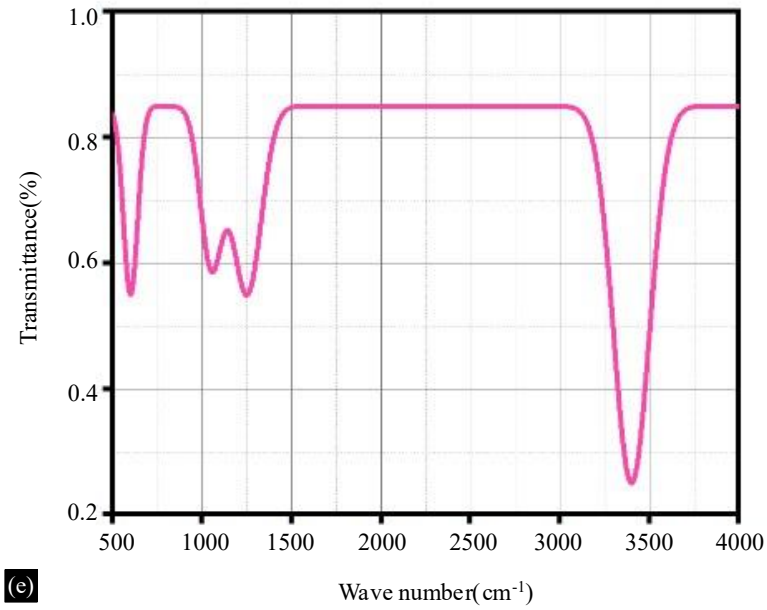

Figure 2. FTIR plots for silicone (a) without doping (b) Doped with TiO_2 (c) Doped with MgO_2 (d) Doped with CaO_2 (e) Doped with ZnO.

Fourier-Transform Infrared (FTIR) spectroscopy is commonly used to investigate chemical bonding and molecular vibrations in organic and inorganic materials. However, pure silver (Ag) is a noble metal and does not exhibit IR-active vibrational modes on its own, due to the lack of permanent dipole moment in metallic bonds and its high reflectivity in the infrared region. The FTIR spectrum of pure silver typically shows no distinct absorption peaks, especially in the fingerprint region (400–1500 cm^{-1}) or the functional group region (1500–4000 cm^{-1}). This is because metallic bonding in silver is non-polar, and FTIR only detects dipole-related vibrations and silver has free electrons that reflect incident IR radiation rather than absorb it. As a result, the spectrum of pure silver appears mostly featureless or flat, with possibly a strong baseline due to reflection or scattering effects, especially if measured as a bulk sample or thin film. Pure silver does not show any IR-active vibrational modes and thus appears nearly inert in FTIR spectroscopy. However, when silver is part of a nanocomposite, functionalized, or oxidized, FTIR can detect indirect spectral features.

FTIR spectroscopy was employed to analyze the chemical interactions, surface modifications, and possible residual organic or oxide layers present on silver-plated copper (Ag/Cu) surfaces. While pure metals like silver and copper are IR-inactive due to their metallic bonding and lack of dipole moment, useful information can still be obtained from surface-bound species, oxides, or residues arising during plating, passivation, or storage. The FTIR spectrum of silver-plated copper typically shows minimal features directly attributable to metallic Ag or Cu. However, secondary features related to surface layers can be observed that weak absorption bands may appear in the region of ~500–650 cm^{-1}, typically due to silver oxide (Ag_2O) or cuprous/cupric oxides (Cu_2O/CuO) on the surface. These oxides can form due to surface oxidation during or after electroplating.

While metallic silver and copper themselves are IR-inactive, FTIR analysis of silver-plated copper surfaces can provide useful insights into surface oxidation, residual organic species from the plating process, moisture or hydroxyl contamination. These surface characteristics are important for electrical, corrosion, and adhesion performance in electronic and microwave applications. Proper surface cleaning or post-processing may be recommended to eliminate residual contaminants.

CONCLUSION

In this study, a comprehensive investigation was conducted on the synthesis, structural characterization, and dielectric performance of polymer-based materials tailored for microwave communication applications. Silicone-based polymer composites, both pure and doped with various metal oxides (TiO_2, MgO_2, CaO_2, ZnO), were successfully synthesized using standard solution casting techniques. Characterization through XRD and FTIR confirmed the incorporation and interaction of the dopants within the polymer matrix, indicating good compatibility and homogeneity. The dielectric measurements revealed that doping significantly influenced the dielectric constant and loss tangent, making it possible to tailor the material properties for specific microwave frequency requirements. Among the doped samples, those with ZnO and TiO_2 exhibited enhanced dielectric properties, such as increased permittivity and reduced dielectric loss, which are essential for efficient signal propagation and minimal attenuation in microwave circuits. These improvements suggest that such composites can serve as promising candidates for high-performance dielectric substrates in antenna design, microwave absorbers, and other RF components. Overall, the study demonstrates the feasibility of modifying polymer matrices through selective doping to achieve desired dielectric behaviors, thereby contributing to the development of next-generation, lightweight, and tunable materials for advanced microwave communication systems.

REFERENCES

1. G. Srilekha, P. Pardhasaradhi, B.T.P. Madhav, et.al. Design and analysis of 6CB nematic liquid crystal–based rectangular patch antenna for S-band and C-band applications, Zeitschrift für Naturforschung A 1 (2020), https://doi.org/ 10.1515/zna-2020-0144.
2. B. Prudhvi Nadh, B.T.P. Madhav, M. Siva Kumar, et.al. Windmill-shaped antenna with artificial magnetic conductor-backed structure for wearable medical applications, Int. J. Numer. Model. 33 (6) (2020), https://doi.org/10.1002/jnm.2757.
3. M. Venkateswara Rao, B.T.P. Madhav, T. Anilkumar, B. Prudhvinadh, circularly polarized flexible antenna on liquid crystal polymer substrate material with metamaterial loading, Microw. Opt. Technol. Lett. 62 (2) (2020) 866–874, https://doi.org/10.1002/mop.32088.
4. Arakawa, Yuki, et al. Effects of alkylthio groups on phase transitions of organic molecules and liquid crystals: a comparative study with alkyl and alkoxy groups. CrystEngComm. 2022; 24(10): 1877-1890.
5. Sharma Anjali, Rijeesh Kizhakidathazhath, and Jan PF Lagerwall. Impact of mesogenic aromaticity and cyano termination on the alignment and stability of liquid crystal shells. Soft Matter. 2023;19(14): 2637-2645.
6. Kim Ho-Gyeom, Jong-Yeong Kim, and Jung-Suek Oh. Design and implementation of an x-band liquid-crystal-based active reflectarray antenna. The Journal of Korean Institute of Electromagnetic Engineering and Science.2021; 32(10): 878-887.

7. Kim Jaehoon, and Jungsuek Oh. Liquid-crystal-embedded aperture-coupled microstrip antenna for 5G applications. IEEE Antennas and Wireless Propagation Letters. 2020; 19(11): 1958-1962.
8. Madhav B. T. P., D. Sreenivas Rao, K. Supraja, et.al. K15 nematic phase liquid crystal material based double-dipole able antenna. Rasayan Journal of Chemistry. 2017; 10(3):866-872.
9. Tejaswi, M., Pardhasaradhi, P., Madhav, B.T.P. et.al. Spectroscopic studies on liquid crystalline pn-nonyloxy benzoic acid (9oba) dispersed citrate capped gold nanoparticles. Optik 2020, 219, p.165151.
10. Ting, T.L. Technology of liquid crystal based antenna. Optics Express 2019, 27(12), pp.17138-17153.
11. Venkateswara Rao M., Madhav, B.T.P., Anilkumar, T. et.al. Circularly polarized flexible antenna on liquid crystal polymer substrate material with metamaterial loading. Microwave and Optical Technology Letters 2020, 62(2), pp.866-874.
12. Du Chengzhu, Xun Wang, and Gao-Ya Jin. A Compact Tri-Band Flexible MIMO Antenna Based on Liquid Crystal Polymer for Wearable Applications. Progress In Electromagnetics Research M 102 (2021): 217-232.
13. H. Eskalen, S. Uruş, and Ş. Özgan. Microwave-assisted synthesis of mushrooms like MWCNT/SiO2@ ZnO nanocomposite: influence on nematic liquid crystal E7 and highly effective photocatalytic activity in degradation of methyl blue. J. Inorg. Organomet. Polym. Mater.2021, vol. 31, no. 2, p. 763.
14. B. P. Singh, S Sikarwar, A.K.Misra et al. Enhanced electro-optical properties of low viscous nematic liquid crystal doped with mixed phase anatase/rutile TiO2 nanoparticles for display applications. World J. Appl. Chem.2021, vol. 6, no. 3, https://doi.org/10.11648/j.wjac.20210603.11.
15. B. P. Singh, S Sikarwar, R.Manohar et al. Nematic liquid crystals blended ferroelectric nanoparticles (BaTiO3): a perspective way for improving the response time and photoluminescence for electro-optical devices. J. Appl. Phys.2022. vol. 131, no. 17, https://doi.org/10.1063/5.0089449.
16. A. Kumar and G. Singh, "Nanoparticles-induced alignment of nematic liquid crystals for tunable electro-optical devices," in Advances in Fabrication and Investigation of Nanomaterials for Industrial Applications, Cham, Springer International Publishing, 2024, pp. 71−89.
17. A. Kouki, F. Sboui, and L. Latrach. Magnetically tuned SIW patch antenna based on nematic liquid crystal for 5G applications and satellite communication systems. Int. J. Microw. Wireless Technol.2023 vol. 15, no. 9, https://doi.org/10.1017/s1759078723000302.
18. D. Kim, K. Kim, H. Kim, et al. Design optimization of reconfigurable liquid crystal patch antenna. Materials.2021. vol. 14, no. 4, https://doi.org/10.3390/ma14040932.
19. J. Kim and J. Oh. Liquid-crystal-embedded aperture-coupled microstrip antenna for 5G applications. IEEE Antenn. Wireless Propag. Lett.2020, vol. 19, no. 11, https://doi.org/10.1109/lawp.2020.3014715.
20. J. Kulkarni, C. Y. D. Sim, A. K. Poddar, et.al. A compact circularly polarized rotated L-Shaped antenna with J-shaped defected ground structure for WLAN and V2X applications. Prog. Electromagn. Res. Lett,2022. vol. 102. https://doi.org/10.2528/pierl22010305.
21. J. Kulkarni and C. Y. D. Sim. Wideband cpw-fed oval-shaped monopole antenna for wi-fi5 and wi-fi6 applications. Prog. Electromagn. Res. C,2021. vol. 107. https://doi.org/10.2528/ pierc20110903.

